

Properties of (μ -Oxo)di-iron Complexes and Catalytic Activity Toward Cyclohexane Oxidation

Gabrieli L. Parrilha,^a Sarah S. Ferreira,^a Christiane Fernandes,^a Giselle C. Silva,^b Nakédia M. F. Carvalho,^b O. A. C. Antunes,^{b,†} Valderes Drago,^c Adailton J. Bortoluzzi^d and Adolfo Horn Jr.*^a

^aLaboratório de Ciências Químicas, Universidade Estadual do Norte Fluminense, 28013-602 Campos dos Goytacazes- RJ, Brazil

^bInstituto de Química, Universidade Federal do Rio de Janeiro, Cidade Universitária, CT Bloco A-641, 21945-970 Rio de Janeiro-RJ, Brazil

^cDepartamento de Física and ^dLaboratório de Bioinorgânica e Cristalografia, Departamento de Química, Universidade Federal de Santa Catarina, 88040-900 Florianópolis-SC, Brazil

Neste artigo são apresentadas a síntese e a caracterização de dois compostos binucleares de ferro, os quais contêm uma ponte μ -oxo. Os compostos $[(SO_4)(L5)Fe(\mu-O)Fe(L5)(SO_4)] \cdot 6H_2O$, **1**, e $[Cl(L5)Fe(\mu-O)Fe(L5)Cl]Cl_2 \cdot 2H_2O$, **2**, foram obtidos nas reações entre 1-(bis-piridin-2-ilmetil-amino)-3-cloropropan-2-ol (L5) e os sais $FeSO_4 \cdot 7H_2O$ e $FeCl_3 \cdot 6H_2O$, respectivamente. Os espectros eletrônicos dos complexos apresentam absorções somente na região do ultravioleta, sendo que a análise eletroquímica revelou que, após a formação da espécie $Fe^{III}Fe^{II}$, a unidade binuclear do composto **1** é mais estável do que a do composto **2**. Os ligantes monodentados (sulfato e cloreto) exercem influência sobre os parâmetros Mössbauer determinados para **1** e **2**, particularmente sobre os desdobramentos de quadrupolo. Os compostos foram empregados como catalisadores em reações de oxidação do cicloexano, usando H_2O_2 e *t*-BuOOH como oxidantes em uma razão substrato:oxidante:catalisador de 1000:1000:1. Os resultados indicam que o composto **2** é um catalisador mais eficiente que o composto **1**.

We report herein the synthesis and characterization of two dinuclear μ -oxo iron compounds obtained through the reactions of $FeSO_4 \cdot 7H_2O$ and $FeCl_3 \cdot 6H_2O$ with 1-(bis-pyridin-2-ylmethyl-amino)-3-chloropropan-2-ol (L5), which resulted in the compounds $[(SO_4)(L5)Fe(\mu-O)Fe(L5)(SO_4)] \cdot 6H_2O$, **1**, and $[Cl(L5)Fe(\mu-O)Fe(L5)Cl]Cl_2 \cdot 2H_2O$, **2**. The electronic spectra of both compounds show absorption bands only in the UV range. The electrochemical analysis showed that the dinuclear unit is more stable under reduction in compound **1** than in compound **2**, while the Mössbauer spectroscopy revealed that the monodentate ligands (sulfate and chloride) have a significant influence on the Mössbauer parameters determined for **1** and **2**, particularly on the quadrupole splitting values. Both compounds were studied as catalysts in reactions of cyclohexane oxidation, using H_2O_2 and *t*-BuOOH as oxidants, in a substrate:oxidant:catalyst ratio of 1000:1000:1. Cyclohexanol, cyclohexanone, cyclohexyl hydroperoxide, *t*-butyl cyclohexyl peroxide and adipic acid were formed during the process. The experiments revealed that compound **2** is, in general, more active than compound **1** in promoting cyclohexane oxidation.

Keywords: di-iron complex, μ -oxo bridge, methane monooxygenase, cyclohexane oxidation

Introduction

Under mild conditions, alkanes are inert compounds in the presence of most chemical reagents due to the

thermodynamic and kinetic stability of their C-C and C-H bonds, which makes their transformation difficult to perform.¹ The evolution of living systems has provided many ways to overcome this difficulty, such as developing different metalloenzymes, like the cytochrome P-450 family and the methane monooxygenases. These are very

[†]Deceased. This paper is dedicated to his memory.

*e-mail: adolfo@uenf.br

specialized systems able to promote specific hydrocarbon oxidation.^{2,3}

Along with copper, iron was selected by nature to form the majority of natural metalloenzymes, which participate in the oxidation of different organic compounds and have inspired several research groups in the search for the so-called biomimetic compounds that have some functional or structural analogies with the natural systems.⁴ In this regard, several heme and non-heme iron complexes have been employed in studies on hydrocarbon oxidation including those of our group.³⁻⁹

Soluble methane monooxygenase (sMMO), which is found in methanotrophic bacteria, is one of the natural systems that promote hydrocarbon oxidation, carrying out the conversion of methane to methanol. The active site of this MMO system contains a di-iron center coordinated to the amino acid residues glutamate and histidine, and to water molecules.⁹ During the sMMO catalytic cycle the oxidation state of the iron ions changes from $\text{Fe}^{\text{II}}\text{-Fe}^{\text{II}}$, the most reduced state, to $\text{Fe}^{\text{IV}}\text{-Fe}^{\text{IV}}$, the most oxidized one. The latter is the main reactive species of the cycle, being responsible for the formation and hydroxylation of alkyl radicals. Intermediate species such as $\text{Fe}^{\text{II}}\text{-Fe}^{\text{III}}$ and $\text{Fe}^{\text{III}}\text{-Fe}^{\text{III}}$ have also been characterized in this catalytic cycle.¹⁰

Several synthetic compounds have been described in the literature as structural and/or functional models for the active site of MMO. For example, the deprotonation of the compound $[\text{Fe}_2(\text{O})(\text{OH})(6\text{tla})_2](\text{ClO}_4)_3$ (6tla = tris(6-methylpyridyl-2-methyl)amine) resulted in the first diamond core bis(μ -oxo)di-iron(III) compound that mimics the sMMO active site containing $\text{Fe}^{\text{III}}\text{Fe}^{\text{III}}$.¹¹ The reaction of $[\text{Fe}_2\text{O}(5\text{-Me-tpa})_2(\text{OH})(\text{H}_2\text{O})](\text{ClO}_4)_3$ (5-Me-tpa = tris(5-methyl-2-pyridylmethyl)amine) with H_2O_2 resulted in a high valence complex containing the $\text{Fe}^{\text{III}}(\text{O})_2\text{Fe}^{\text{IV}}$ unit, which has also been characterized by spectroscopic and structural methods and is claimed to be analogous to the intermediate Q observed in the catalytic cycle of MMO.¹² Other di-iron complexes have been synthesized as models for the sMMO peroxo intermediate.¹³ From the catalytic point of view, a number of mono and dinuclear iron complexes have been studied in reactions of hydrocarbon oxidation.^{7,8,14-16} In general, cyclohexane is the first substrate chosen as a model, because its manipulation and transformation is much easier than that of methane. Furthermore, the products obtained from cyclohexane oxidation, cyclohexanol and cyclohexanone, are precursors to adipic acid and caprolactam, which have extensive industrial applications in Nylon-6 and Nylon-66 manufacturing. Due to the high amount of energy expended in the actual process, the development of catalytic systems that operate under mild conditions is desired.¹⁷

In order to contribute to a better understanding of how different ligand groups affect the physicochemical and structural properties of coordination compounds, we have recently published the synthesis and characterization of a family of mononuclear iron complexes containing bis(2-pyridylmethyl)amine derivative ligands (Figure 1: L1- L4). Results showing the reactivity of these iron compounds with H_2O_2 and O_2 , as well as their use as catalysts in cyclohexane oxidation, were reported.^{8,18-20} Following this same line, we report herein the synthesis and characterization of two new dinuclear iron complexes $[(\text{SO}_4)(\text{L5})\text{Fe}(\mu\text{-O})\text{Fe}(\text{L5})(\text{SO}_4)]\cdot 6\text{H}_2\text{O}$, **1**, and $[\text{Cl}(\text{L5})\text{Fe}(\mu\text{-O})\text{Fe}(\text{L5})\text{Cl}]\text{Cl}_2\cdot 2\text{H}_2\text{O}$, **2**, which were synthesized with a new member of the bis(2-pyridylmethyl)amine family: L5 = 1-(bis-pyridin-2-ylmethyl-amino)-3-chloropropan-2-ol (Figure 1). An alcohol function was incorporated into this ligand aiming to compare its coordination ability with the ligands that possess amide (L3) and carboxylate (L4) groups. Both complexes **1** and **2** had their catalytic activity in cyclohexane oxidation investigated. The synthesis, molecular structure and nuclease activity of **1** have been published previously.²¹

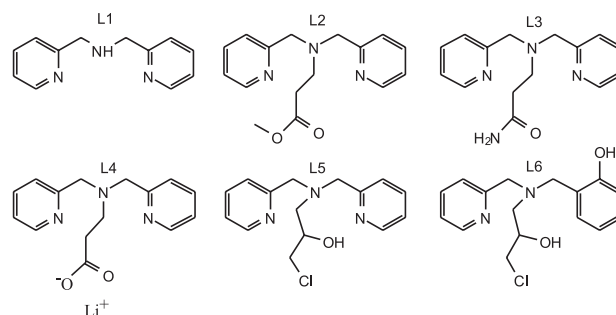


Figure 1. Family of ligands containing the bis(2-pyridylmethyl)amine unit (L1-L5). The structure for ligand L6 is included because it is discussed in the text.

Results and Discussion

Syntheses

The complexes were synthesized according to the scheme in Figure 2. During the preparation of **1**, a very small amount of a brown solid was formed, which was eliminated by filtration. In the synthesis of **2**, immediate precipitation of a yellow solid was observed after the addition of the iron salt to the solution containing L5. We tried to isolate this product, but it is highly deliquescent. An initial characterization of this yellow solid, performed by infrared spectroscopy, revealed the absence of Fe-O-Fe stretching, indicating that it might be a mononuclear iron complex. This difficulty, concerning the isolation of a stable solid,

was solved by refluxing. However, with this procedure, only a red solid could be isolated, characterized as a (μ -oxo)di-iron compound. Interestingly, it was observed that the use of L5 results in dinuclear μ -oxo iron compounds, while the other members of this family (L1-L4) produce mononuclear iron compounds under similar reaction conditions. We have previously published the synthesis of copper and manganese compounds with L5. For these metal ions, only mononuclear compounds were isolated.^{22, 23}

Both iron complexes are soluble only in polar solvents, including water, MeOH, CH₃CN, dimethylformamide (DMF) and dimethylsulfoxide (DMSO). Conductivity analysis revealed that both compounds behave as electrolytes in water, indicating that, at least for **1** and under the conditions employed, the sulfate group should be displaced from the iron coordination environment.

X-ray molecular structure

The ellipsoid plots of the molecular structure of complexes **1** and **2** are presented in Figure 3, the main bond distances and angles are shown in Table 1 and the crystallographic data are given in Table 2.

The molecular structure of **1** has been published previously. Compound **1** shows a neutral dinuclear unit with the iron(III) ions connected by a μ -oxo bridge (Fe-O-Fe = 163.2(3) $^\circ$). Each iron(III) ion is also coordinated by one L5 ligand molecule and one monodentate sulfate ion, resulting in a N₃O₃ coordination environment around the metal centers.

The bis(2-pyridylmethyl)amine units from the ligand molecules adopt a meridional coordination mode (Fe-N_{amine}: average = 2.236 Å, Fe-N_{py}: average = 2.138 Å), with the pyridine groups *trans* to each other. The same coordination mode was observed in mononuclear copper complexes synthesized with L5;²² however, it differs from the mononuclear seven-coordinate manganese compound, in which the pyridine groups are in *cis* arrangement.²³

Although it is recognized that the oxo bridge exerts a significant *trans* effect, it is not very pronounced in **1**, since the Fe-N_{amine} bond lengths (*ca.* 2.23 Å) are in the range observed for iron compounds containing tertiary amines *cis*

to the oxo bridge. For example, the Fe-N_{amine} bond lengths in the compound [(tpa)(OH)FeOFe(H₂O)(tpa)]³⁺ (tpa = tris(2-pyridylmethyl)amine) are 2.194(8) Å when the N is *cis* to the oxo bridge and 2.264(8) Å when it is *trans*. In the compound [(tpa)ClFeOFeCl(tpa)]²⁺, the aliphatic nitrogen atoms are *cis* to the oxo bridge and the Fe-N bond distances are 2.227(6) Å.²⁴ For the complex [(trispicMeen)ClFeOFeCl(trispicMeen)], where trispicMeen = *N,N,N'*-tris-(2-pyridylmethyl)-*N'*-methylethane-1,2-diamine, the N_{amine} *trans* to the oxo bridge shows an Fe-N bond length of 2.270(16) Å, while the N_{amine} atoms *cis* to μ -O the values are 2.243(15) and 2.261(12) Å.²⁵

In **1** the alcohol groups are located *trans* to the monodentate sulfate group and *cis* to the oxo bridge. The Fe-O_{alcohol} distances (average: 2.140 Å) indicate that the alcohol group is protonated. Also, its hydrogen atoms were found from the Fourier difference map. The Fe-O_{alcohol} (*ca.* 2.140 Å) and Fe-N_{pyridine} (2.138 Å) bond lengths are very similar, indicating that, at least in terms of structural parameters, both groups have similar basicity.

The cation **2** lies on a crystallographic inversion center and, accordingly, it has exact C_i local symmetry, which gives the chloride ions an *anti* configuration, similar to that observed in the compound [(tpa)ClFeOFeCl(tpa)]²⁺.²⁴ In complex **1**, in its turn, the sulfate groups show a *syn* configuration. The L5 coordination mode also differs significantly from that observed in **1**. In **1** the N_{amine} atoms are *trans* to the oxo bridge, while in **2** the alcohol groups occupy this position. In contrast, the N_{amine} in **2** is *cis* to the oxo bridge, with Fe-N_{amine} distances of 2.191(3) Å. The pyridyl groups are positioned *trans* to each other, as observed in **1**.

In **2**, the Fe-O-Fe unit is linear, which makes the Fe...Fe distance (3.580(5) Å) slightly longer than in **1** (3.5323(13) Å). The oxo bridge in **2** shows a more pronounced *trans* effect when compared with **1**, resulting in a Fe-O_{alcohol} bond length of 2.241(2) Å. This bond distance was approximately 2.140 Å in **1**, with the alcohol coordinated *cis* to the oxo bridge. Curiously, although there are different groups *trans* to the oxo bridge in **1** (amine) and **2** (alcohol), the bond lengths are practically the same: 2.236(5) in **1** and 2.241(2) Å in **2**. The Fe-N bond lengths in **2** are slightly shorter than in **1**.

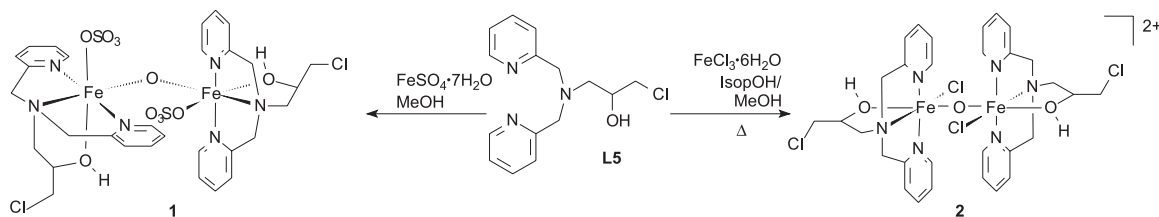


Figure 2. Synthesis of compounds **1** and **2**.

Both isomeric forms of the ligand are observed in **2** (*R* around Fe1i and *S* around Fe1), while only the *R* isomer is present in **1**.

We have previously reported the coordination behavior of a similar ligand {*N*-(2-hydroxybenzyl)-*N*-(2-pyridylmethyl) [(3-chloro)(2-hydroxy)] propylamine} (L6 in Figure 1) which differs from L5 by the presence of one pyridine and one phenol group instead of two pyridines as observed in L5. L6 forms a mononuclear compound when it reacts with $\text{FeCl}_3 \cdot 6\text{H}_2\text{O}$,⁸ while dinuclear iron complexes were obtained by reactions with $\text{FeSO}_4 \cdot 7\text{H}_2\text{O}$ and $\text{Fe}(\text{ClO}_4)_3 \cdot 9\text{H}_2\text{O}$. The structural characterization of the dinuclear complexes synthesized with L6, $[\text{Fe}_2(\text{L6})_2(\text{H}_2\text{O})_2]^{2+}$, $[\text{Fe}_2(\text{L6})_2(\text{OAc})]^+$ and $[\text{Fe}_2(\text{L6})_2(\text{SO}_4)]$,²⁶ revealed that the iron ions are bridged by alkoxide groups from the ligand instead of presenting an oxo bridge, as observed for **1** and **2**.

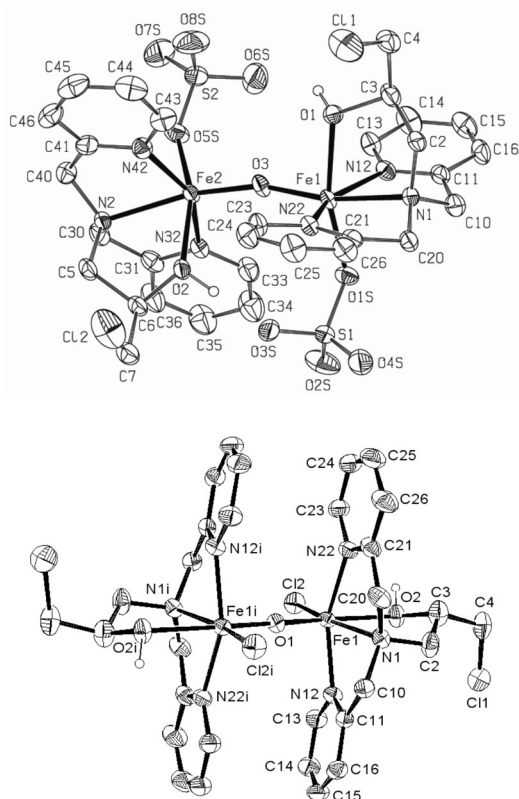


Figure 3. ORTEP diagrams for **1** (top) and **2** (bottom) with thermal ellipsoids at 40% probability. Hydrogen atoms and solvates are omitted for clarity. Symmetry code for **2**: $-x, -y, -z+1$.

Spectroscopic and electrochemical characterization

The infrared spectra of the complexes are very similar, with the major difference being related to the presence of sulfate groups in **1**, resulting in bands at 1175, 1124, 1106 and 1036 cm^{-1} . Bands characteristic of pyridine groups are observed at 1610, 1573, 1487 and 1449 cm^{-1} ,

Table 1. Selected bond lengths and angles for complexes **1** and **2**

Complex 1		Bond lengths (\AA)	
Fe1-O3	1.777(4)	Fe2-O3	1.793(4)
Fe1-O1S	1.961(4)	Fe2-O5S	1.958(4)
Fe1-N12	2.140(5)	Fe2-N32	2.120(5)
Fe1-O1	2.144(4)	Fe2-O2	2.135(4)
Fe1-N22	2.145(5)	Fe2-N42	2.146(6)
Fe1-N1	2.235(5)	Fe2-N2	2.237(5)
Angles ($^\circ$)			
O3-Fe1-O1S	104.6(2)	O3-Fe2-O5S	108.71(19)
O3-Fe1-N12	103.7(2)	O3-Fe2-N32	105.0(2)
O1S-Fe1-N12	86.96(19)	O5S-Fe2-N32	87.1(2)
O3-Fe1-O1	90.58(18)	O3-Fe2-O2	89.78(18)
O1S-Fe1-O1	163.84(18)	O5S-Fe2-O2	161.20(18)
N12-Fe1-O1	84.06(19)	N32-Fe2-O2	84.72(19)
O3-Fe1-N22	103.89(19)	O3-Fe2-N42	102.2(2)
O1S-Fe1-N22	93.02(19)	O5S-Fe2-N42	88.4(2)
N12-Fe1-N22	151.5(2)	N32-Fe2-N42	152.4(2)
O1-Fe1-N22	88.56(18)	O2-Fe2-N42	91.04(19)
O3-Fe1-N1	167.0(2)	O3-Fe2-N2	165.05(19)
O1S-Fe1-N1	88.38(19)	O5S-Fe2-N2	86.11(19)
N12-Fe1-N1	76.53(19)	N32-Fe2-N2	76.9(2)
O1-Fe1-N1	76.48(17)	O2-Fe2-N2	75.55(17)
N22-Fe1-N1	75.00(19)	N42-Fe2-N2	75.7(2)
Complex 2		Bond lengths (\AA)	
Fe1-O1	1.7897(5)	Fe1-N1	2.191(3)
Fe1-N12	2.121(3)	Fe1-O2	2.241(2)
Fe1-N22	2.123(3)	Fe1-Cl2	2.2758(9)
Angles ($^\circ$)			
O1-Fe1-N12	92.69(8)	N22-Fe1-O2	82.69(11)
O1-Fe1-N22	92.79(8)	N1-Fe1-O2	76.28(10)
N12-Fe1-N22	153.88(12)	O1-Fe1-Cl2	104.59(3)
O1-Fe1-N1	92.60(8)	N12-Fe1-Cl2	100.93(8)
N12-Fe1-N1	76.27(11)	N22-Fe1-Cl2	102.35(9)
N22-Fe1-N1	77.99(12)	N1-Fe1-Cl2	162.74(8)
O1-Fe1-O2	168.63(7)	O2-Fe1-Cl2	86.60(7)
N12-Fe1-O2	87.03(11)	Fe1-O1-Fe1i	180.00(5)

and of the alcohol group at 3450 cm^{-1} . The asymmetric stretching of the oxo bridge ($\nu_{\text{as}} \text{Fe-O-Fe}$) gives rise to a band of medium intensity at 832 for **1** and 825 cm^{-1} for **2**, presenting higher wavenumber values when compared with $[(\text{tpa})\text{ClFeOFeCl}(\text{tpa})]^{2+}$ ($\nu_{\text{as}} = 816 \text{ cm}^{-1}$).²⁴

The Mössbauer spectra of the complexes were collected at room temperature (Figure 4). The spectra for both complexes consist of a single quadrupole doublet, indicating the presence of only one type of iron

Table 2. Crystal data and structure refinement for complexes **1** and **2**

	Complex 1	Complex 2
Empirical formula	C ₃₀ H ₄₈ Cl ₂ Fe ₂ N ₆ O ₁₇ S ₂	C ₃₀ H ₄₀ Cl ₆ Fe ₂ N ₆ O ₅
Formula weight	1011.46	889.08
Temperature (K)	293(2)	293(2)
Wavelength (Å)	0.71073	0.71073
Crystal system	Monoclinic	Triclinic
Space group	P 2/c	P $\bar{1}$
Unit cell dimensions		
a (Å)	19.104(4)	8.4405(7)
b (Å)	15.071(3)	10.2902(12)
c (Å)	16.826(3)	12.4575(16)
α (°)		66.714(3)
β (°)	108.81(3)	84.629(3)
γ (°)		72.324(3)
Volume (Å ³)	4585.6(16)	946.50(18)
Z	4	1
Density (calc.) (Mg/m ³)	1.465	1.560
μ (mm ⁻¹)	0.911	1.236
F(000)	2096	456
Crystal size (mm ³)	0.40 × 0.26 × 0.23	0.24 × 0.18 × 0.10
Theta range (°)	1.13 to 25.08	3.56 to 26.05
Index ranges	-22 ≤ h ≤ 0; 0 ≤ k ≤ 17; -18 ≤ l ≤ 20	-10 ≤ h ≤ 10; -12 ≤ k ≤ 12; -15 ≤ l ≤ 15
Reflections collected	8380	10816
Independent reflections	8124 [R(int) = 0.0249]	3709 [R(int) = 0.0227]
Absorption correction	Psi-scan	Multiscan
Transmission factors	0.808 and 0.769	0.886 and 0.756
Refinement method	Full-matrix least-squares on F ²	Full-matrix least-squares on F ²
Data / parameters	8124 / 502	3709 / 233
Goodness-of-fit on F ²	1.090	1.053
R indices [I > 2σ(I)]	R ₁ = 0.0681, wR ₂ = 0.1985	R ₁ = 0.0488, wR ₂ = 0.1272
R indices (all data)	R ₁ = 0.1387, wR ₂ = 0.2171	R ₁ = 0.0594, wR ₂ = 0.1329

nucleus in the solid state for each complex. The observed isomer shifts (δ 0.34 for **1** and δ 0.32 mm s⁻¹ for **2**) are characteristic of high spin iron(III). The quadrupole splitting values (ΔE_q = 1.67 for **1** and ΔE_q = 0.98 mm s⁻¹ for **2**) indicate that the iron atoms possess an anisotropic electronic environment. Since high spin Fe^{III} centers show a dependence of ΔE_q on the local symmetry and on the electronic environment,²⁷ the higher value of ΔE_q obtained for compound **1** might be related to a less symmetric coordination environment around the iron ions or it might reflect the presence of dianionic sulfate ions, which have a very distinct basicity when compared with the chloride ions coordinated in **2**.

The electronic spectra of the complexes in CH₃CN solution are very similar (Figure 5). One band and two

shoulders were observed for complex **1** and two bands and one shoulder for complex **2**, all of them located in the UV range and presenting ϵ values typical of charge transfer transitions. The band of highest energy is located near 255 nm (ϵ ca. 21 × 10³ dm³ mol⁻¹ cm⁻¹) for both complexes, and is attributed to ligand-centered transitions (pyridine). The shoulders between 300 and 400 nm observed in the spectra of **1** can be attributed to oxo → Fe^{III} LMCT transitions.²⁸

Complex **2** also shows a band at 339 (ϵ = 6.5 × 10³ dm³ mol⁻¹ cm⁻¹) and a shoulder near 400 nm (ϵ = 3.5 × 10³ dm³ mol⁻¹ cm⁻¹). Similar bands have also been observed in mononuclear iron compounds containing chloride coordinated to iron(III) ions, and were assigned to LMCT Cl → Fe^{III}.¹⁸ Since complex **2** possesses both oxo and

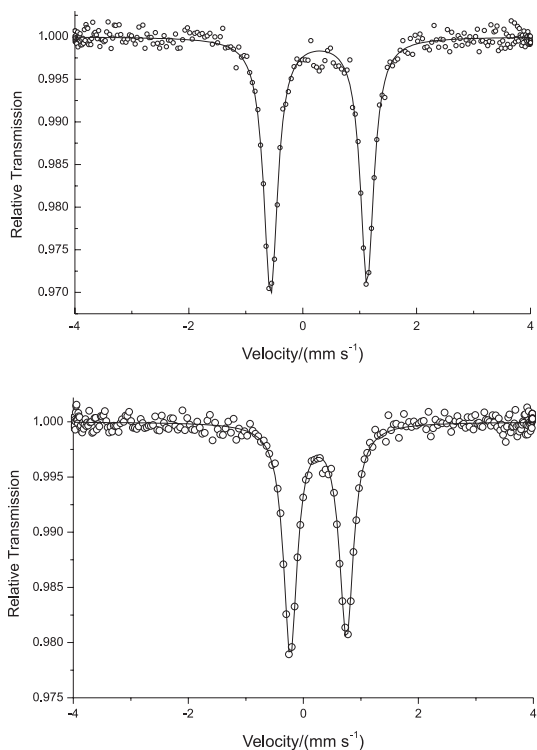


Figure 4. Mössbauer spectra for compounds **1** (top) and **2** (bottom).

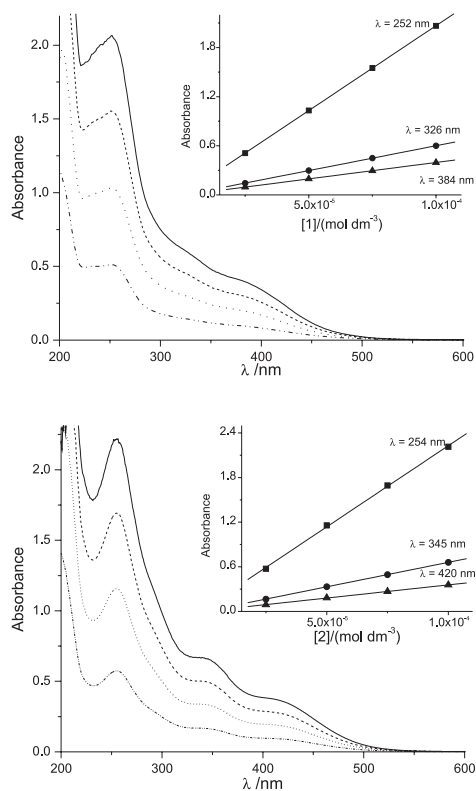


Figure 5. Electronic spectrum of **1** (top) and **2** (bottom) in acetonitrile at different concentrations: (—) 1.0×10^{-4} ; (---) 7.5×10^{-5} ; (···) 5.0×10^{-5} and (---) 2.5×10^{-5} mol dm^{-3} . λ_{max} (nm) / ϵ ($\text{dm}^3 \text{mol}^{-1} \text{cm}^{-1}$): **1** = 252/2.1 $\times 10^4$; 326/6.1 $\times 10^3$; 384/4.0 $\times 10^3$. **2** = 254/2.2 $\times 10^4$; 345/6.6 $\times 10^3$; 420/3.5 $\times 10^3$. The insets show the plots of A versus [complex], used to calculate the ϵ values.

chloride ligands coordinated to iron(III), it is possible that the absorptions observed between 300 and 450 nm are composed of LMCT $\text{Cl} \rightarrow \text{Fe}^{\text{III}}$ and $\text{oxo} \rightarrow \text{Fe}^{\text{III}}$.

Both complexes show no distinct absorption features in the visible range, which is characteristic of complexes containing linear Fe-O-Fe units. Hence, it is possible to hypothesize that the Fe-O-Fe core in **1** might show a linear Fe-O-Fe arrangement in solution,²⁹ although in the solid state its angle is 163°.

The cyclic voltammograms of **1** and **2** are rather distinct (Figure 6). The internal standard Fc/Fc^+ is observed at 0.418 V ($\Delta E_p = 125$ mV), and the free L5 base does not show any electrochemical process between -1.8 to 1.0 V.

Compound **1** shows two *quasi*-reversible redox processes at -0.690 ($\Delta E_p = 0.151$ V) and -1.30 V ($\Delta E_p = 0.222$ V) associated with the redox couples $\text{Fe}^{\text{III}}\text{Fe}^{\text{III}}/\text{Fe}^{\text{III}}\text{Fe}^{\text{II}}$ and $\text{Fe}^{\text{III}}\text{Fe}^{\text{II}}/\text{Fe}^{\text{II}}\text{Fe}^{\text{II}}$. Furthermore, it is possible to see another oxidation wave at -0.322 V *versus* Fc/Fc^+ , which means that the anodic wave for the first redox process, observed at -0.690 V *vs.* Fc/Fc^+ , is associated with two oxidative processes. A similar behavior has been observed for the compound [(trispicMeen)ClFe^{III}OFe^{III}Cl(trispicMeen)]²⁺,²⁵ for which the anodic process for the first redox couple was composed of two oxidation waves attributed to the presence of two species in equilibrium, a six and a five coordinated Fe^{II} . Since a similar feature is observed in the cyclic voltammogram of **1**, the presence of two species in equilibrium can be proposed. Thus, after the first process of reduction, the sulfate anion possibly leaves the coordination environment of the iron center and six and five coordinated iron(II) ions coexist on the electrode surface, resulting in the two anodic processes.

The cyclic voltammogram of **2** shows two very well defined irreversible processes, one cathodic at -0.426 and another anodic at -0.223 V *versus* Fc/Fc^+ . There is a second irreversible cathodic process with low current intensity at -0.826 V *vs.* Fc/Fc^+ . The electrochemical profile presented by **2** is similar to that reported by Costes and co-workers.³⁰ For (L)Fe-O-Fe(L) compounds, where L is a Schiff base, Costes suggested that, after the first step of reduction - which leads to the formation of the mixed valence $\text{Fe}^{\text{III}}\text{Fe}^{\text{II}}$ - the dinuclear unit is broken, resulting in mononuclear species that are oxidized at a more positive potential. Thus, it is possible to hypothesize that there is a chemical reaction associated with the reduction process of **2** at -0.426 V, resulting in the breaking of the dinuclear unit and formation of mononuclear species. This explains why the electrochemical behavior of **2** is so distinct from that of **1**. The presence of a second cathodic process with low current intensity may suggest that a small amount of the dinuclear unit remains on the electrode surface.

The anodic process observed at -0.223 V is related to the oxidation of the mononuclear iron(II) species

electrochemically formed on the electrode surface. The formation of this mononuclear species is also supported by the fact that the anodic wave at -0.223 V is in the range observed for the mononuclear iron compounds containing L1 ($E_{1/2} = -0.347$ V *versus* Fc/Fc⁺), L2 ($E_{1/2} = -0.257$ V *versus* Fc/Fc⁺) and L3 ($E_{1/2} = -0.222$ V *versus* Fc/Fc⁺).

Comparing the molecular structures of **1** and **2**, it is possible to explain their distinct electrochemical behaviors. For **1**, the alcohol group bound to one of the iron centers has an orientation that allows it to form a hydrogen bond with the sulfate group bound to the other iron center and/or with the oxo bridge. On the other hand, the alcohol groups present in **2** are coordinated *trans* to the oxo bridge, which does not allow any kind of interaction with the groups coordinated to the second iron center. Thus, the lack of intramolecular hydrogen bonding in **2** could lead to the rupture of the dinuclear unit after reduction, while for **1** it is proposed that the intramolecular hydrogen bond is responsible for the maintenance of the dinuclear structure.

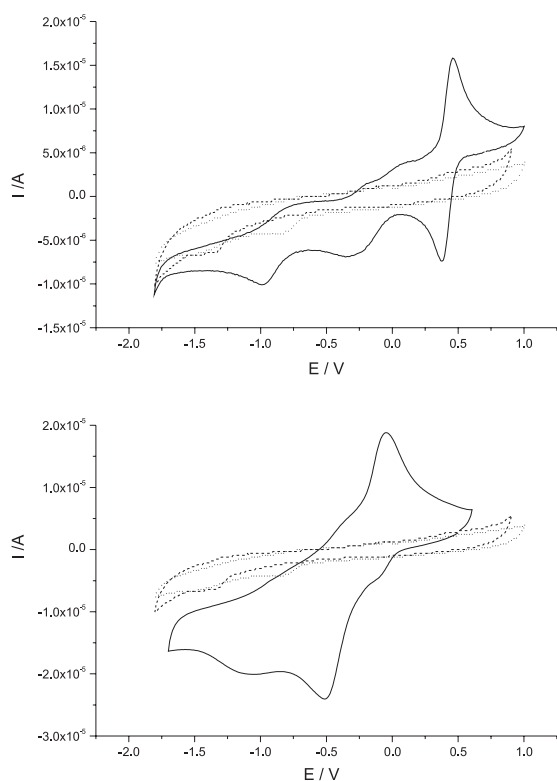
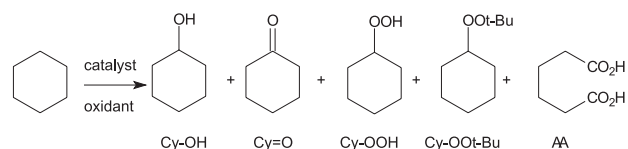


Figure 6. Cyclic voltammograms for compounds **1** (top) and **2** (bottom) under argon atmosphere. Ferrocene was used as internal standard for complex **1** and as external standard for complex **2**. Scan rate: 100 mV s⁻¹. Support electrolyte: 0.1 mol dm⁻³ solution of tetrabutylammonium perchlorate in acetonitrile. Pseudo-reference electrode: Pt wire. (---) base line, (····) ligand, (—) complex

Cyclohexane oxidation

Since the molecular structures of **1** and **2** are dinuclear and a dinuclear iron core is present at the methane monooxygenase

active site, experiments aiming to evaluate whether the complexes could have monooxygenase activity were carried out. Cyclohexane was employed as the substrate and the reactions were performed employing different solvents (MeCN/BuOH), oxidants (hydrogen peroxide or *tert*-butylperoxide) and temperatures (25 and 50 °C). Cyclohexanol (Cy-OH), cyclohexanone (Cy=O), cyclohexyl hydroperoxide (Cy-OOH), *t*-butyl cyclohexyl peroxide (Cy-OO*t*-Bu) and adipic acid (AA) were formed during the oxidation process (Scheme 1, Table 3). Control reactions were carried out in the absence of the catalysts and no oxidation products were observed. It is also important to note that the yields reported in Table 3 were based on the substrate, since other kinds of reactions (catalase activity, insertion of oxo groups in the structure of the complexes etc.) may take place.



Scheme 1. Products observed during cyclohexane oxidation promoted by compounds **1** and **2**. Cy-OH: cyclohexanol; Cy=O: cyclohexanone; Cy-OOH: cyclohexyl hydroperoxide; Cy-OO*t*-Bu: *tert*-butylcyclohexyl peroxide; AA: adipic acid.

At 25 °C, employing acetonitrile as the solvent and H₂O₂ as the oxidant (Table 3, entry 1), complex **2** was more active than complex **1**. Adipic acid was the main product obtained for complex **2**, followed by Cy-OOH, Cy-OH and Cy=O. Interestingly, adipic acid is virtually absent when complex **1** is used, indicating that the two complexes have different behaviors in promoting the cyclohexane oxidation under these conditions.

Interestingly, when the temperature is raised to 50 °C (Table 3, entry 2) the total conversions observed for **1** and **2** are similar. Under this condition, the product adipic acid was not observed, differing significantly from the results obtained at lower temperature, mainly for complex **2**. For **1**, the main product obtained is Cy-OOH, while, for complex **2**, Cy=O was obtained in larger amounts. This suggests that a different oxidation pathway may be in place.

When the oxidant was changed from H₂O₂ to *t*-BuOOH, practically no oxidation was observed at 25 °C (Table 3, entry 3), but it reaches 19% (**1**) and 16% (**2**) at 50 °C (Table 3, entry 4). Under this condition, results indicate the same trend concerning the oxidation products for both complexes, and the major product formed is Cy=O, which suggests that the catalytic species should be the same for the two precursors. Furthermore, this result reveals that the temperature has an important effect on both the yield and oxidation mechanism. The influence of the temperature was also observed for compound **1** when H₂O₂ was employed

as the oxidant (Table 3, entry 1). Entries 3 and 4 indicate that the interaction between the catalysts and the oxidants (mainly for *t*-BuOOH) would not occur so easily at room temperature, probably due to some steric hindrance, since it is facilitated at 50 °C. Thus, it is possible to suggest that, at the higher temperature (50 °C), the coordination environment of the iron center changes (ligand exchange or rupture of the dinuclear unit), facilitating the catalyst-oxidant interaction, which results in a higher yield for the oxidation reaction.

The change of solvent from acetonitrile to *t*-BuOH had a negative effect on the total conversion for both temperatures and oxidants. Firstly, we decided to study the cyclohexane oxidation in *t*-BuOH due to the fact that both complexes **1** and **2** are insoluble in this solvent. Thus, a heterogeneous catalysis could take place. However, the addition of the oxidants to the complexes made them soluble, resulting in a homogeneous system. When H₂O₂ was used as the oxidant (entries 5 and 6) a very low amount of oxidation products were observed at room temperature. However, at 50 °C, complex **2** showed the highest selectivity toward cyclohexanol.

The system *t*-BuOOH/*t*-BuOH (Table 3, entries 7 and 8) gives reasonable results only at 50 °C for complex **2**. Under these conditions complex **2** showed the highest production and selectivity for Cy=O.

The two complexes presented here are less effective in promoting cyclohexane oxidation than the mononuclear iron complexes synthesized with the ligands L1-L4 and L6.^{7,8} In contrast to this tendency, Li and co-workers³¹ reported similar results in the cyclohexane oxidation when the mononuclear [Fe(tpoen)Cl]PF₆ and the dinuclear [{Fe(tpoen)}₂(μ -O)](ClO₄)₄ compounds were employed as catalysts (tpoen = *N*-(2-pyridylmethoxyethyl)-*N,N*-bis(2-pyridylmethyl)amine). On the other hand, the dinuclear iron compound [Fe₂OL₂(MeOH)₂(NO₃)₂](NO₃)₂ (L = 2,6-bis(*N*-methylbenzimidazol-2-yl)pyridine) was able to promote the cyclohexane oxidation while the mononuclear iron compound with the same ligand, [FeLCl₃], was inactive. Compounds **1** and **2** showed lower activity than the compounds [{Fe(tpoen)}₂(μ -O)](ClO₄)₄ and [Fe₂OL₂(MeOH)₂(NO₃)₂](NO₃)₂.

Several effects may account for the oxygenase activity of the iron compounds: the redox potential, the lability of the ligands, the presence of ligands able to form hydrogen bonds and steric hindrance effects.³²⁻³⁴ The analysis of our data reveals that compounds **1** and **2** are very distinct catalysts. The activity of each compound is dependent on the experimental conditions (solvent, temperature, oxidant) employed in the oxidation reaction. Since both are dinuclear μ -oxo compounds and contain the same polydentate ligand, the differences observed in the reactivity may be related to the following points: *i*) the

coordination mode of the polydentate ligand around the iron ions; *ii*) the charges and types of the monodentate ligands (SO₄²⁻ and Cl⁻); *iii*) the charges presented by the complexes; *iv*) the redox potential of the metal center. Since several variables can be related to each other, at the present time it is not possible to establish the factors which drive the activity of the iron complexes synthesized with the ligand L5.

Considering the molecular structure, in compound **2** the chloro ligands show an *anti* configuration to each other, while in **1**, the sulfate ions are *syn*. This structural difference may explain the higher activity of compound **2**, since the iron centers in this compound are more accessible to the oxidant than those in **1**. Furthermore, electrochemical data showed that the dinuclear unit in **2** is not very stable. Since we have observed previously that the mononuclear iron compounds synthesized with L1-L4 and L6 are more active in cyclohexane oxidation than the dinuclear compounds presented here, it is possible that the easier conversion of the dinuclear **2** in a mononuclear compound makes this complex a better catalyst than compound **1**.

Conclusions

This study revealed that the tripodal tetradentate ligand L5 yields the formation of (μ -oxo)di-iron(III) compounds. This feature is independent of the oxidation state of the iron salt employed in the synthesis (Fe^{II} or Fe^{III}). However, the behaviors related to the coordination mode of the ligand differ, and this accounts for the distinct electrochemical behaviors and probably to the catalytic activities. In general, compound **2** was more effective than compound **1** in promoting cyclohexane oxidation, although the results for both complexes showed a dependence on the reaction conditions (solvent, oxidant, temperature). The two complexes were more active in the medium with H₂O₂ as the oxidant and acetonitrile as the solvent at 50 °C, furnishing the highest turnover values under these conditions. Complexes **1** and **2** showed lower activity than the mononuclear complexes synthesized with the ligands L1-L4 and L6. The presence of a more labile ligand (chloride), the lower steric hindrance, as well as the higher propensity to form mononuclear compounds observed for compound **2**, can be considered to explain its higher activity as a catalyst for oxygenation reactions when compared with **1**.

Experimental

Materials and methods

Reagents and solvents were used as received from commercial sources. Only the solvents used for electrochemical and electronic spectroscopy analyses were of spectroscopic grade. L5 was synthesized as described previously.²²

Table 3. Results for the cyclohexane oxidation catalyzed by complexes **1** and **2** after 24 h

Entry	T (°C)	Oxidant	Solvent	Catalyst	Yield (%) ^a						Cy-OH/ Cy=O	TN ^b
					Cy-OH	Cy=O	Cy-OOH	Cy-OO <i>t</i> -Bu	AA	Total		
1	rt	H ₂ O ₂	ACN	1	1.0	-	5.6	-	-	6.6	-	72
				2	2.9	1	5.7	-	7.7	17.3	2.9	173
2	50	H ₂ O ₂	ACN	1	5.4	3.5	12.6	-	-	21.5	1.5	217
				2	3.9	11.2	2.8	-	-	17.9	0.35	185
3	rt	<i>t</i> -BuOOH	ACN	1	1	-	-	-	-	1	-	23
				2	-	-	-	-	-	-	-	-
4	50	<i>t</i> -BuOOH	ACN	1	5.9	9.4	2.2	1.4	-	18.9	0.63	191
				2	5.5	8.3	1.0	1.1	-	15.9	0.66	161
5	rt	H ₂ O ₂	<i>t</i> -BuOH	1	-	-	-	-	-	-	-	-
				2	-	-	2.1	-	1	3.1	-	38
6	50	H ₂ O ₂	<i>t</i> -BuOH	1	1	-	1.2	-	-	2.2	-	27
				2	5.6	2.9	-	-	1	9.5	1.9	92
7	rt	<i>t</i> -BuOOH	<i>t</i> -BuOH	1	-	-	-	-	-	-	-	-
				2	-	-	-	-	6.8	6.8	-	73
8	50	<i>t</i> -BuOOH	<i>t</i> -BuOH	1	1.4	1.5	1.9	-	-	4.8	0.9	55
				2	2.6	11.6	-	2.3	-	16.5	0.22	167

^aYields were calculated in relation to the substrate, using the equation (1), which relates the yield calculated from chromatographic analysis and the yield calculated from titration. For the chromatographic yield, the equations (2) and (3) were employed, using the corrected areas of the products (considering the corresponding response factor). ^b TN, turnover number; calculated as mol of products *per* mol of catalyst. $R_t = R_{AA} + R_{rc}$ (1), where R_t = total yield; R_{AA} = yield of adipic acid obtained from titration; R_{rc} = corrected chromatographic yield; $R_{rc} = \frac{R_c \times n_c}{n_t}$ (2), where R_c = chromatographic yield; n_c = number of moles analyzed by GC ($n_c = n_t - n_{aa}$; n_{aa} = mols of adipic acid; n_t = number of moles of substrate); $R_c = \frac{A_p}{A_t} \times 100$ (3), where A_p = corrected area of the products from GC; A_t = total corrected area (sum of the areas of products and substrate from GC).

UV-Vis spectra were recorded on a Shimadzu 1601PC UV-Vis spectrophotometer in acetonitrile. Infrared spectra were collected on a FTIR Nicolet Magna-IR 760 spectrophotometer, with the sample dispersed in KBr. Mössbauer spectra were obtained using a Wissel instrument in the constant acceleration mode with transmission geometry. A ⁵⁷Co/Rh source was maintained at room temperature. The resultant spectra were least-squares fitted to Lorentzian shaped lines using the NORMOS software (Wissel Company). Metallic iron was used for energy calibration and also as a reference for the isomer shift (δ) scale. Conductivity measurements were carried out with solutions containing 1×10^{-3} mol dm⁻³ of the complexes, using a BioCristal NT CVM conductivimeter, employing a conductivity cell CA150. Cyclic voltammetry experiments were carried out using an Autolab PGSTAT10 potentiostat/galvanostat and a three electrode system, with a glassy carbon disk as the working electrode, a platinum wire as the auxiliary electrode and a platinum wire as the pseudo-reference electrode. As the supporting electrolyte, a 0.1 mol dm⁻³ solution of tetrabutylammonium perchlorate in acetonitrile was used. The redox couple Fc/Fc⁺ (0.400 V *versus* NHE) was used as the internal standard.³⁵ Cyclohexane was purified before handling through successive extractions with H₂SO₄, H₂O and NaHCO₃ solution (1%), respectively,

and distilled over CaH₂. The oxidants, H₂O₂ and tert-butyl hydroperoxide (*t*-BuOOH), were titrated using the iodometric method. The oxidation products were analyzed in an HP 5890 gas chromatographer with FID detector and a DB-5 column.

Synthesis of $[(SO_4)(L5)Fe(\mu-O)Fe(L5)(SO_4)] \cdot 6H_2O$ (**1**)

This complex was obtained through the reaction of a methanolic solution (50 cm³) of L5 (2 mmol, 0.58 g) followed by the addition of an equimolar amount of solid FeSO₄·7H₂O (0.56 g). The solution acquired immediately a greenish-brown color. The reaction mixture was stirred for one hour, filtered and left to stand. The next day a red microcrystalline material began to precipitate. After 3 days, this microcrystalline solid was filtered, washed with cold propan-2-ol and dried under vacuum (0.48 g, 48%). Found: C, 33.95; H, 4.9; N, 7.6; C₃₀H₃₆Cl₂Fe₂N₆O₁₁S₂·9H₂O requires C, 33.8; H, 5.1; N, 7.9%. IR (KBr) ν_{max} /cm⁻¹: 3463 (OH), 1610, 1573, 1487, 1449 (C=C, C=N, pyridine), 1175, 1124, 1106, 1036 (SO₄), 832 (Fe-O-Fe). $\Lambda_M = 22.7$ cm² Ω⁻¹ mol⁻¹ (DMF: no electrolyte).³⁶ This solid was recrystallized in MeOH, rendering red diamond shaped crystals suitable for X-ray analysis.

Synthesis of $[Cl(L5)Fe(\mu-O)Fe(L5)Cl]Cl_2 \cdot 2H_2O$ (**2**)

2 mmol (0.58 g) of L5 were dissolved in 20 cm³ of propan-

2-ol, followed by the addition of a solution (propan-2-ol, 20 cm³) containing an equimolar amount of FeCl₃·6H₂O. A yellow solid was immediately formed. Methanol (50 cm³) was added and the solution was refluxed for 1.5 h, rendering an orange solution. This solution was kept at room temperature, and after four days red single crystals suitable for X-ray analysis were isolated (0.39 g, 44%). Found: C = 40.5; H = 4.4; N, 9.3; C₃₀H₃₆Cl₆Fe₂N₆O₃·2H₂O requires C = 40.5; H = 4.5; N = 9.45. IR (KBr) ν_{max} /cm⁻¹: 3421 (OH), 1607, 1570, 1483, 1445 (C=C, C=N, pyridine), 825 (Fe-O-Fe). $\Lambda_{\text{M}} = 147.8 \text{ cm}^2 \Omega^{-1} \text{ mol}^{-1}$ (DMF: 2:1 electrolyte type).³⁶

Crystallographic analysis

Crystallographic analysis was carried out on a CAD-4 diffractometer for complex **1** and on an APEX II diffractometer for complex **2**, at room temperature. For complex **1**, the electronic density attributed to highly disordered solvent molecules was removed using squeeze correction with PLATON.³⁷ All non-hydrogen atoms were refined with anisotropic displacement parameters, except for the oxygen atoms of the six water molecules of crystallization. Hydrogen atoms attached to carbon atoms were fixed at their idealized positions, whereas the H atoms of the alcohol groups were found from the Fourier map and treated with a riding model. The hydrogen atoms for the water molecules were not found. For complex **2**, all non-hydrogen atoms were refined anisotropically. The counterion chloride (Cl⁻) is disordered over two alternative positions, with refined occupancy of 0.52(5) and 0.48(5). H atoms of the alcohol group and of the water molecule were found from the Fourier map and also treated with a riding model. Other H atoms were placed at their idealized positions, with C-H distances and U_{eq} values taken from the default settings of the refinement program. Further crystallographic information is given in Table 2.

Cyclohexane oxidation

The reactions were carried out in a 50 cm³ round bottom flask under stirring for 24 h. Different solvents, temperatures and oxidants were employed, using an experimental optimization method. The catalyst:substrate:oxidant ratio was 1:1000:1000. The reagent amounts were: 0.75 cm³ of cyclohexane (7×10^{-3} mol), 0.59 cm³ of H₂O₂ or 0.93 cm³ of *t*-BuOOH (7×10^{-3} mol), 7.4 mg of **1** or 6.0 mg of **2** (7×10^{-6} mol). Acetonitrile (MeCN) and *t*-butanol (*t*-BuOH) were used as the solvents (10 cm³) and the experiments were carried out at two temperatures: room temperature (25 °C) and 50 °C. The reactions were quenched by the addition of an aqueous 0.4 mol dm⁻³ solution of Na₂SO₄, followed by extraction with 10 cm³ of diethyl ether. The ether layer was

dried with anhydrous Na₂SO₄ and analyzed by GC. Retention times and mass spectra compared with standards were used to characterize most of the reaction products. Yields were calculated taking into account the different response factors to FID of the substrate (cyclohexane) and products (cyclohexanol and cyclohexanone) through external standardization. For cyclohexyl hydroperoxide, the response factor to FID was considered to be the same as that of cyclohexanol. The aqueous phase was titrated with NaOH to quantify the total acid compounds obtained in the reaction, expressed as adipic acid.

Supplementary Information

The crystallographic data (atomic coordinates and equivalent isotropic displacement parameters, calculated hydrogen atom parameters, anisotropic thermal parameters and bond lengths and angles) have been deposited at the Cambridge Crystallographic Data Center (deposition numbers CCDC 672086 and CCDC 672087). Copies of this information may be obtained free of charge from: CCDC, 12 Union Road, Cambridge, CB2 1EZ, UK (Fax: +44-1223-336-033; e-mail: deposit@ccdc.cam.ac.uk or <http://www.ccdc.cam.ac.uk>).

Acknowledgments

The authors are grateful for the financial support received from CNPq (Jovens Pesquisadores and INCT-Catálise), CAPES, FAPERJ (Jovem Cientista do Nosso Estado, Pronex) and FUJB. The authors also thank Dr. Manfredo Hörner and Dr. Robert A. Burrow (Departamento de Química, Universidade Federal de Santa Maria) for the crystallographic facilities use.

References

1. Crabtree, R. H.; *Chem. Rev.* **1995**, *95*, 987.
2. Denisov, I. G.; Makris, T. M.; Sligar, S. G.; Schlichting, I.; *Chem. Rev.* **2005**, *105*, 2253.
3. Costas, M.; Chen, K.; Que, L. Jr.; *Coord. Chem. Rev.* **2000**, *200*, 517; Tshuva, E. Y.; Lippard, S. J.; *Chem. Rev.* **2004**, *104*, 987; Bois, J. D.; Mizoguchi, T. J.; Lippard, S. J.; *Coord. Chem. Rev.* **2005**, *200*, 443.
4. Que Jr., L.; Tolman, W. B.; *Nature* **2008**, *455*, 333.
5. Tang, J.; Gamez, P.; Reedijk, J.; *Dalton Trans.* **2007**, 4644; Pan, Z.; Newcomb, M.; *Inorg. Chem.* **2007**, *46*, 6767; Nam, W.; Jin, S. W.; Lim, M. H.; Ryu, J. Y.; Kim, C.; *Inorg. Chem.* **2002**, *41*, 3647; Halma, M.; Bail, A.; Wypych, F.; Nakagaki, S.; *J. Mol. Catal. A: Chem.* **2006**, *243*, 44; Nakagaki, S.; Castro, K. A. D. F.; Machado, G. S.; Halma, M.; Drechsel, S. M.; Wypych, F.; *J. Braz. Chem. Soc.* **2006**, *17*, 1672; Wada, A.; Ogo, S.; Nagatomo, S.; Kitagawa, T.; Watanabe, Y.; Jitsukawa, K.; Masuda, H.; *Inorg. Chem.* **2002**,

- 41, 616; England, J.; Britovsek, G. J. P.; Rabadia, N.; White, A. J. P.; *Inorg. Chem.* **2007**, *46*, 3752.
6. Olsen, M. H. N.; Salomão, G. C.; Drago, V.; Fernandes, C.; Horn, A. Jr.; Cardozo-Filho, L.; Antunes, O. A. C.; *J. Supercrit. Fluids* **2005**, *34*, 119; Salomão, G. C.; Olsen, M. H. N.; Drago, V.; Fernandes, C.; Cardozo-Filho, L.; Antunes, O. A. C.; *Catal. Commun.* **2007**, *8*, 69; Esmelindro, M. C.; Oestreicher, E. G.; Márquez-Alvarez, H.; Dariva, C.; Egues, S. M. S.; Fernandes, C.; Bortoluzzi, A. J.; Drago, V.; Antunes, O. A. C.; *J. Inorg. Biochem.* **2005**, *99*, 2054.
7. Carvalho, N. M. F.; Horn, A. Jr.; Antunes, O. A. C.; *Appl. Catal., A* **2006**, *305*, 140.
8. Silva, G. C.; Parrilha, G. L.; Carvalho, N. M. F.; Drago, V.; Fernandes, C.; Horn, A. Jr.; Antunes, O. A. C.; *Catal. Today* **2008**, *133*, 684.
9. Rosenzweig, A. C.; Frederick, C. A.; Lippard, S. J.; Nordlund, P.; *Nature* **1993**, *366*, 537; Whittington, D. A.; Lippard, S. J.; *J. Am. Chem. Soc.* **2001**, *123*, 827.
10. Basch, H.; Mogi, K.; Musaev, D. G.; Morokuma, K.; *J. Am. Chem. Soc.* **1999**, *121*, 7249.
11. Zang, Y.; Dong, Y.; Que, L. Jr.; Kauffmann, K.; Muenck, E.; *J. Am. Chem. Soc.* **1995**, *117*, 1169.
12. Dong, Y.; Fujii, H.; Hendrich, M. P.; Leising, R. A.; Pan, G.; Randall, C. R.; Wilkinson, E. C.; Zang, Y.; Que, L. Jr.; Fox, B. G.; Kauffmann, K.; Münck, E.; *J. Am. Chem. Soc.* **1995**, *117*, 2778; Hsu, H. F.; Dong, Y.; Shu, L.; Young, V. G. Jr.; Que, L. Jr.; *J. Am. Chem. Soc.* **1999**, *121*, 5230.
13. Kryatov, S. V.; Taktak, S.; Korendovych, I. V.; Rybak-Akimova, E. V.; Kaizer, J.; Torelli, S.; Shan, X.; Mandal, S.; MacMurdo, V. L.; Payeras, A. M.; Que, L. Jr.; *Inorg. Chem.* **2005**, *44*, 85; Kim, S. O.; Sastri, C. V.; Seo, M. S.; Kim, J.; Nam, W.; *J. Am. Chem. Soc.* **2005**, *127*, 4178; Li, F.; Wang, M.; Ma, C.; Gao, A.; Chen, H.; Sun, L.; *Dalton Trans.* **2006**, 2427; Zhang, X.; Furutachi, H.; Fujinami, S.; Nagatomo, S.; Maeda, Y.; Watanabe, Y.; Kitagawa, T.; Suzuki, M.; *J. Am. Chem. Soc.* **2005**, *127*, 826.
14. Pardo, E.; Lloret, F.; Carrasco, R.; Muñoz, M. C.; Temporal-Sánchez, T.; Ruiz-García, R.; *Inorg. Chim. Acta* **2004**, *357*, 2713.
15. Britovsek, G. J. P.; England, J.; White, A. J. P.; *Inorg. Chem.* **2005**, *44*, 8125.
16. Carson, E. C.; Lippard, S. J.; *Inorg. Chem.* **2006**, *45*, 837; Britovsek, G. J. P.; England, J.; Spitzmesser, S. K.; White, A. J. P.; Williams, D. J.; *Dalton Trans.* **2005**, 945; Nan, W.; *Acc. Chem. Res.* **2007**, *40*, 522.
17. Schuchardt, U.; Cardoso, D.; Sercheli, R.; Pereira, R.; Cruz, R. S.; Guerreiro, M. C.; Mandelli, D.; Spinacé, E. V.; Pires, E. L.; *Appl. Catal., A* **2001**, *211*, 1.
18. Carvalho, N. M. F.; Horn, A. Jr.; Bortoluzzi, A. J.; Drago, V.; Antunes, O. A. C.; *Inorg. Chim. Acta* **2006**, *359*, 90.
19. Carvalho, N. M. F.; Horn, A. Jr.; Faria, R. B.; Bortoluzzi, A. J.; Drago, V.; Antunes, O. A. C.; *Inorg. Chim. Acta* **2006**, *359*, 4250.
20. Carvalho, N. M. F.; Antunes, O. A. C.; Horn, A. Jr.; *Dalton Trans.* **2007**, 1023.
21. Parrilha, G. L.; Fernandes, C.; Bortoluzzi, A. J.; Szpoganicz, B.; Silva, M. S.; Pich, C. T.; Terenzi, H.; Horn, A. Jr.; *Inorg. Chem. Commun.* **2008**, *11*, 643.
22. Horn, A. Jr.; Fernandes, C.; Bortoluzzi, A. J.; Vugman, N. V.; Herbst, M. H.; *J. Mol. Struct.* **2005**, *749*, 96; Fernandes, C.; Parrilha, G. L.; Lessa, J. A.; Santiago, L. J. M.; Kanashiro, M. M.; Boniolo, F. S.; Bortoluzzi, A. J.; Vugman, N. V.; Herbst, M. H.; Horn, A. Jr.; *Inorg. Chim. Acta* **2006**, *359*, 3167.
23. Lessa, J. A.; Horn, A. Jr.; Pinheiro, C. B.; Farah, L. L.; Eberlin, M. N.; Benassi, M.; Catharino, R. R.; Fernandes, C.; *Inorg. Chem. Commun.* **2007**, *10*, 863.
24. Hazell, A.; Jensen, K. B.; Mckenzie, C. J.; Toftlund, H.; *Inorg. Chem.* **1994**, *33*, 3127.
25. Nivorozhkin, A. L.; Anxolabéhère-Mallart, E.; Mialane, P.; Davydov, R.; Guilhem, J.; Cesario, M.; Audière, J.-P.; Girerd, J.-J.; Styring, S.; Schussler, L.; Seris, J.-L.; *Inorg. Chem.* **1997**, *36*, 846.
26. Horn, A. Jr.; Neves, A.; Vencato, I.; Drago, V.; Zucco, C.; Werner, R.; Haase, W.; *J. Braz. Chem. Soc.* **2000**, *11*, 7; Horn, A. Jr.; Vencato, I.; Bortoluzzi, A. J.; Horner, R.; Silva, R. A. N.; Szpoganicz, B.; Drago, V.; Terenzi, H.; de Oliveira, M. C. B.; Werner, R.; Haase, W.; Neves, A.; *Inorg. Chim. Acta* **2005**, *358*, 339; Horn, A. Jr.; Vencato, I.; Bortoluzzi, A. J.; Drago, V.; Novak, M. A.; Neves, A.; *J. Braz. Chem. Soc.* **2006**, *17*, 1584.
27. Greenwood, N. N.; Gibb, T. C.; *Mössbauer Spectroscopy*, Chapman and Hall: London, 1971.
28. Marchi-Delapierre, C.; Jorge-Robin, A.; Thibon, A.; Ménage, S.; *Chem. Commun.* **2007**, 1166; Nagataki, T.; Tachi, Y.; Itoh, S.; *J. Mol. Catal. A: Chem.* **2005**, *225*, 103; Taktak, S.; Kryatov, S. V.; Rybak-Akimova, E. V.; *Inorg. Chem.* **2004**, *43*, 7196.
29. Wilkinson, E. C.; Dong, Y.; Que, L. Jr.; *J. Am. Chem. Soc.* **1994**, *116*, 8394; Ito, S.; Okuno, T.; Matsushima, H.; Tokii, T.; Nishida, Y.; *J. Chem. Soc., Dalton Trans.* **1996**, 4037; Norman, R. E.; Holz, R. C.; Ménage, S.; O'Connor, C. J.; Zhang, J. H.; Que, L. Jr.; *Inorg. Chem.* **1990**, *29*, 4629.
30. Costes, J.-P.; Tommasino, J.-B.; Carré, B.; Soulet, F.; Fabre, P.-L.; *Polyhedron* **1995**, *14*, 771.
31. Li, F.; Wang, M.; Ma, C.; Gao, A.; Chen, H.; Sun, L.; *Dalton Trans.* **2006**, 2427.
32. Wang, X.; Wang, S.; Li, L.; Sundberg, E. B.; Gacho, G. P.; *Inorg. Chem.* **2003**, *42*, 7799.
33. Leising, R. A.; Kim, J.; Pérez, M. A.; Que, L. Jr.; *J. Am. Chem. Soc.* **1993**, *115*, 9524.
34. Ito, S.; Okuno, T.; Matsushima, H.; Tokii, T.; Nishida, Y.; *J. Chem. Soc., Dalton Trans.* **1996**, 4479.
35. Gagne, R. R.; Koval, C. A.; Lisensky, G. C.; *Inorg. Chem.* **1980**, *19*, 2854.
36. Geary, W.; *Coord. Chem. Rev.* **1971**, *7*, 81.
37. Spek, A. L.; *Acta Crystallogr., Sect. A: Found. Crystallogr.* **1990**, *46*, C34.

Received: March 31, 2009

Web Release Date: December 11, 2009